Density Fluctuations and Energy Spectra of 3D Bacterial Suspensions Supplemental Material

Zhengyang Liu, Wei Zeng, Xiaolei Ma, and Xiang Cheng
Department of Chemical Engineering and Materials Science, University of Minnesota, Minneapolis, MN 55455, USA
(Dated: December 20, 2020)

I. MATERIALS AND METHODS

A. Light-powered *E. coli*

We introduce a light-driven transmembrane proton pump, proteorhodopsin (PR), to wild-type *E. coli* (BW25113) by transforming the bacteria with plasmid pZE-PR encoding the SAR86 γ-proteobacterial PR-variant (Walter 2007). The activity of PR is correlated with the intensity of light. Thus, we can control the swimming speed of bacteria using light of different intensities. In our experiments, we use high-intensity light, which saturates the light response of bacteria. The average swimming speed of bacteria is fixed at $v_0 = 15 \pm 3$ μm/s in the dilute limit.

The bacteria are cultured at 37 ℃ with a shaking speed at 250 rpm for 14-16 hours in terrific broth (TB) [tryptone 1.2% (w/w), yeast extract 2.4% (w/w), and glycerol 0.4% (w/w)] supplemented with 0.1 g/L ampicillin. The culture is then diluted 1:100 (v:v) in fresh TB and grown at 30 ℃ for 6.5 hours. PR expression is triggered by supplementing the culture medium with 1 mM isopropyl β-D-thiogalactoside and 10 μM ethanolic all-trans-retinal in the mid-log phase, 3 hours after the dilution.

The bacteria are harvested by gentle centrifugation (800g for 5 min). After discarding the culture medium in the supernatant, we resuspend bacteria with DI water. The resuspended suspension is then centrifuged again at 800g for 5 min, and finally adjusted to the target concentration for experiments.

B. Sample preparation and microscopy

To prepare the sample for microscopy, we construct a seal chamber made of glass slides (25 mm × 75 mm) and coverslips (18 mm × 18 mm). We first glue (NOA 81, Norland, NJ) two coverslips on a glass slide, side-by-side, leaving a 3-mm separation between the two coverslips. We then cover the 3-mm separation with another coverslip to form a channel. We then pipette bacterial suspensions into the channel. Finally, we seal the two ends of the channel using UV glue (NOA 76, Norland, NJ) to form a sealed chamber.

Images of the bacterial suspensions are taken 50 μm above the bottom surface of the sealed chamber by a Nikon Ti-E inverted microscope using the bright field mode with a 20× (NA 0.5) objective. The field of view is 420 × 360 μm^2. All videos are recorded at 30 frames per second using a sCMOS camera.

II. IMAGE ANALYSIS

A. Density fluctuations

1. *Pixel intensity and bacterial number*

In Fig. 1d, we show that under the same illumination and imaging condition, bacterial density and the average pixel intensity follow approximately a linear relation, which can be expressed as follows:

$$\phi = a + bI, \tag{1}$$

where ϕ is the volume fraction of bacterial suspensions, I is the average pixel intensity, a and b are constants under the same illumination and imaging condition. The number of bacteria in a given subsystem with side length l and thickness d can be calculated as

$$N = \frac{l^2 d}{V_b}\phi = \frac{l^2 d}{V_b}(a + bI), \tag{2}$$

where V_b is the volume of a single bacterium. d is the depth of the field of microscopy, which is fixed in our experiments. We estimate $d \approx XX$ μm. Yi approximated it to be about 10 μm. But I am not sure if he has any solid evidence on the number. Thus, the number of bacteria in the subsystem N is proportional to $l^2\phi$. Taking the standard deviation of both sides of Eq. 2, we get

$$\Delta N = \frac{l^2 d}{V_b}|b|\Delta I, \tag{3}$$

where ΔN and ΔI are the standard deviation of the bacterial number and the standard deviation of the average pixel intensity of the subsystem over time, respectively. Since $d|b|/V_b$ is a constant independent of subsystem sizes and bacterial volume fractions, ΔN is linearly proportional to $l^2\Delta I$. Because any constant in front of ΔN would not affect either the scaling relation or the relative magnitude of density fluctuations at different ϕ, we simply use $l^2\Delta I$ as ΔN in our study.

2. *Density fluctuations at different length scales*

Based on the linear relation between ΔN and ΔI, we calculate the density fluctuations at different length

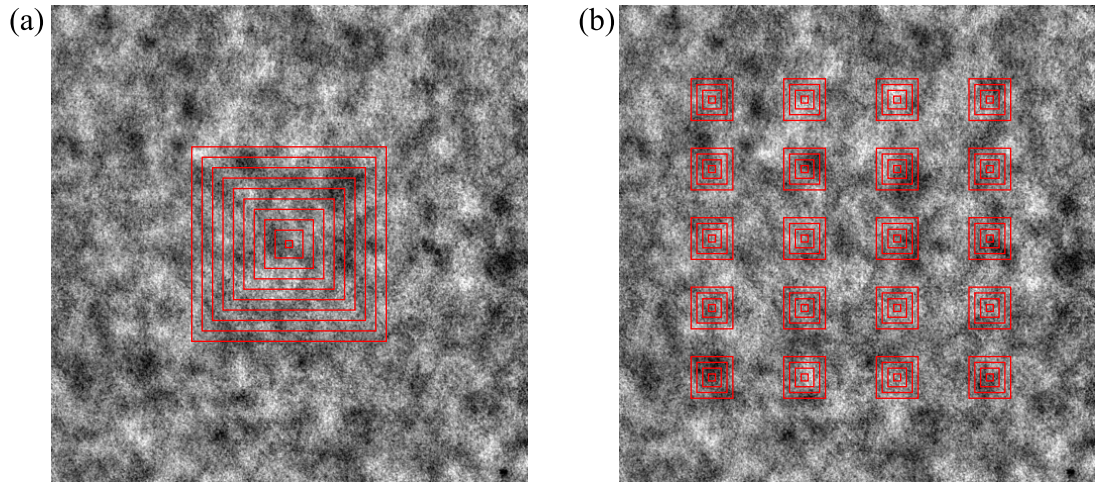

FIG. 1. **GNF calculations.** (a) Varying subsystem sizes. (b) Multiple seeds of subsystems for spatial average.

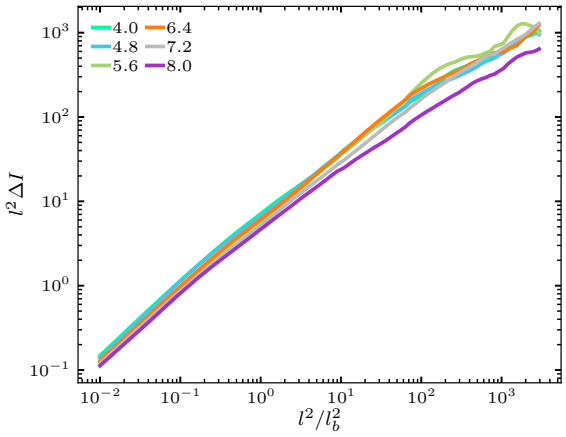

FIG. 2. **GNF curves at various volume fractions under same illumination and imaging conditions.**

scales. We first crop square-shape subsystems of increasing sizes, as shown in Fig. 1a. For each subsystem size l, the standard deviation of the average pixel intensity of the subsystem is calculated over 50 frames (1.67 s or $8.35\tau_b$), which is longer than the saturated density correlation time (Fig. 2f). To improve statistics, we choose 20 subsystems of the same size evenly distributed in the field of view and obtain a spatial average of the temporal standard deviation of the average pixel intensity ΔI (Fig. 1b). This averaged ΔI is then multiplied by l^2 to give the number density fluctuations ΔN at the length scale l. Note that a second method has also been proposed for calculating number fluctuations, where the standard deviation of bacterial numbers is computed first spatially over different locations in a single time frame and is then averaged over time of different frames []. Although the two methods lead to the same results when spatial and temporal correlations are small compared with the system size and experiment duration [], the second method is subject to a systematic error due to potential stable non-uniform light illumination in our experiments. Hence, we use the first method introduced above in our study. Using this method, any non-uniform stable light illumination would result in a zero temporal standard deviation of I and, therefore, would not affect our measurement of true density fluctuations. I am not sure it is necessary to show Fig. 1. Furthermore, it is a little confusing to show two figures with subsystems of different sizes. We can discuss if and how to present the figures better.

3. *Normalization of bacterial suspensions of different volume fractions*

Practically, to optimize image qualities, we adjust the exposure time of imaging for suspensions of different ϕ. Exposure times may affect the proportional constant b in Eq. 1, which then introduces a ϕ-dependent linear constant $b(\phi)$ in Eq. 2. Although $b(\phi)$ would not change the scaling exponent of the density fluctuations α at each given ϕ, it will affect the relative magnitude of ΔN at different ϕ. In order to compare the magnitude of density fluctuations at different ϕ, we further calibrate and normalize ΔI for different ϕ. Specifically, as the calibration, we fix the intensity of illumination and the exposure time and take videos of bacterial suspensions at different ϕ under the exact same imaging condition. The calibration results are shown in Fig. 2, where all the curves at different ϕ collapse at small length scales. First, why we don't see the diffusive behavior at large l in this plot? Second, I am not sure if I agree with the argument below. Our density-fluctuation measurements show bacterial correlation at small scales even in dilute suspensions. Thus, we cannot detect only single bacterial dynamics at small

scales. If that was the case, we should see $\Delta I l^2$ become flat as we discussed before. The observation is intuitive: small scale density fluctuations is determined primarily by single cell dynamics and is not a strong function on volume fractions. Based on the calibration, we normalize $l^2\Delta I$ by its value at a fixed small length scale. We choose the small scale at $l = 0.3l_b$ in our study. However, since $l^2\Delta I$ at different ϕ shows the same slope at small l, choosing any other small lengths between XXl_b and XXl_b would lead to quantitatively the same results. After the normalization, the density fluctuations measured in our experiments show not only the correct scaling exponent but also the right relative magnitude at different ϕ.

B. Particle image velocimetry (PIV)

2D in-plane velocity fields are extracted by Particle Image Velocimetry (PIV) analysis using the openPIV package in Python [1]. We fix the box size to be 16 μm, which is larger than the size of a single bacterial body but smaller than the velocity correlation length. A step size of the half of the box size (8 μm) is used by convention, which sets the spatial resolution of the velocity fields.

C. Energy spectra

The energy spectra of bacterial suspensions are calculated as follows. First, we apply the built-in Fast Fourier Transform (FFT) function of Python `numpy.fft` package to convert the discrete velocity field $\boldsymbol{v}(\boldsymbol{r}) = [v_x(x,y), v_y(x,y)]$ obtained from PIV to the velocity field in the momentum k space $\boldsymbol{v_k}(\boldsymbol{k}) = [u_k(k_x,k_y), v_k(k_x,k_y)]$. Thanks for clarifying the details on how to do FFT including the step size and 2π factor. We should certainly document it in your thesis, but I don't think we need to put the details in the paper. The point-wise kinetic energy density in the k-space is then computed as

$$E(k_x,k_y) = \frac{1}{2A}\langle u_k(k_x,k_y)u_k^*(k_x,k_y) + v_k(k_x,k_y)v_k^*(k_x,k_y)\rangle \quad (4)$$

where A is the total area of the field of view and * denotes the complex conjugate. Why is $2A$ not A? The $\langle\cdot\rangle$ indicates an average over multiple images from different times. Finally, the energy spectrum $E(k)$ is obtained by summing up $E(k_x,k_y)$ at a constant $k = (k_x^2+k_y^2)^{1/2}$. I don't think this is exactly what you do. If I am right, you average $E(k_x,k_y)$ in a small ring and then calculate $E(k) = 2\pi k$ times the average $E(k_x,k_y)$. The two approaches are the same mathematically.

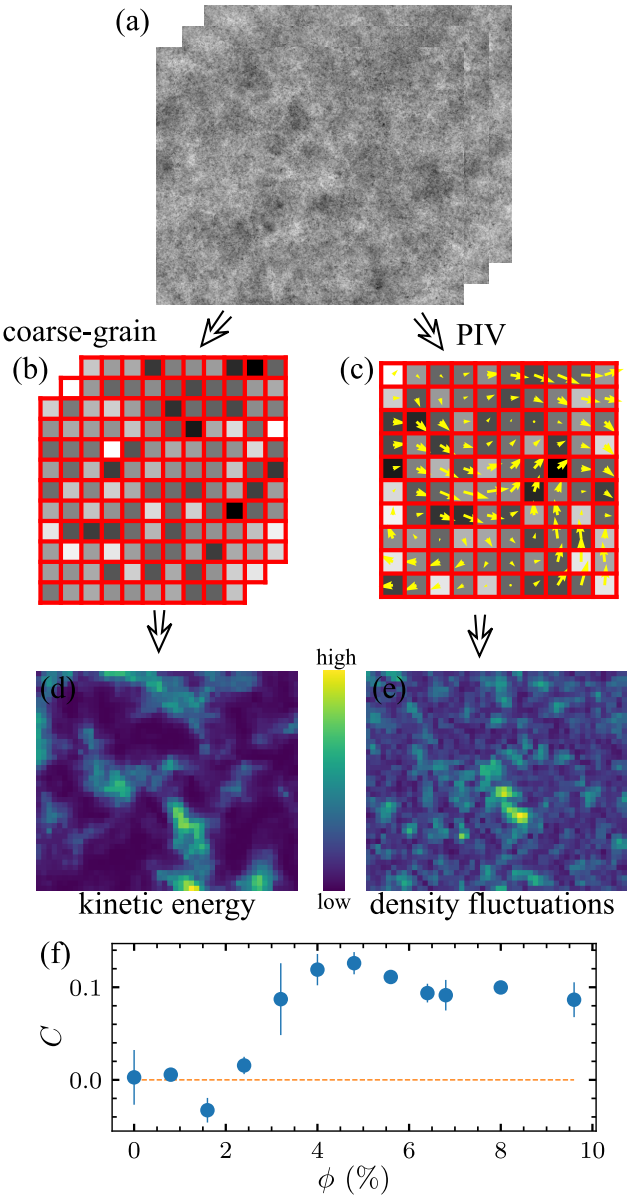

FIG. 3. Diagram showing the procedures of calculating local coupling between density fluctuations and kinetic energy.

D. Correlation of local density fluctuations and kinetic energies

To calculate local temporal density fluctuations, we need to approximate instantaneous intensity variations. On the one hand, the time interval for calculating the intensity difference between two frames needs to be smaller than the density correlation time in order to satisfy the instantaneous approximation, which is typically around 2 s (60 frames), as shown in Fig.**??**. where does the 2 s comes from? The correlation is $4\tau_b$, which is 0.8 s. On the other hand, the time interval should be sufficient long to suppress the influence of random fluctuations of im-

age intensities in adjacent frames, a factor that always needs to be considered when calculating the derivative of an experimental quantity. In our study, we choose 0.3 s (10 frames) for the local density fluctuation calculation. We do not expect the results to be much different when varying this number from 0.17 to 0.6 s.

I am not clear about the procedure below. What's $F_i(\boldsymbol{r})$? Is it the intensity field? Where is the length scale $l = 2.5l_b$ we stated in the main text? Is $2.5l_b = 8$ μm? The way you calculate kinetic energies is quite different from what I thought (if I understand your procedure right). Why not do PIV on the original images without coarsen-graining and then calculate the kinetic energies with a window by summing up velocity squares in that window. Will that give you the same result? We don't need to show 3f, since it is already in the main text. As shown in Fig. 3, we first take 10 frames $F_i(\boldsymbol{r})$ of consecutive images, where $i = 1, 2, ..., 10$. All the 10 frames are coarse-grained by binning 25×25 px^2 (8×8 μm^2) windows into a single pixel $f_i(\boldsymbol{r})$, as shown in Fig. 3b. PIV algorithm is then applied on the first two images to obtain a representative velocity field $v\boldsymbol{r}$, as in Fig. 3c. Since the PIV analysis is done at a step size of 25 pixel, the coarse-graining procedure produces images with dimensions the same as the velocity fields obtained from PIV. We then take the standard deviation of the pixel intensity at each spot over 10 frames to obtain a field of density fluctuations, $\delta N(\boldsymbol{r}) = \sqrt{\langle (f_i - \langle f_i \rangle)^2 \rangle}$, shown in Fig. 3d. The kinetic energy field is obtained by taking square of the magnitudes of PIV result and then divide it by 2, $E_k(\boldsymbol{r}) = v(\boldsymbol{r})^2/2$, as shown in Fig. 3e. Finally, the normalized correlaiton between $\Delta N(\boldsymbol{r})$ and $E_k(\boldsymbol{r})$ is calculated as

$$C = \frac{\langle (\Delta N - \overline{\Delta N})(E_k - \overline{E_k}) \rangle}{\sigma_{\Delta N} \sigma_{E_k}} \tag{5}$$

where $\bar{\cdot}$ means taking the mean, σ means the standard deviation, and $\langle \cdot \rangle$ denotes taking the average of all scalars in an array. The cross correlation quantifies the similarity between arrays N and E_k. The resulting number takes value from -1 to 1.

E. Density fluctuations in the transient state

Density fluctuations in the transient state towards active turbulence is calculated using the same method as that in the steady state. Specifically, the procedure described in Sec. II A is applied at time t over a time interval of Δt during the transition towards active turbulence. We choose $\Delta t = 1.7$ s (50 frames), which is slightly smaller than the density correlation time and thus provides sound statistics. As a comparison, the entire transition takes about 60 s (1800 frames). Thus, Δt is also small enough and provides a good temporal resolution to monitor the kinetic process.

$\widetilde{l}^2$

[1] A. Liberzon, D. Lasagna, M. Aubert, P. Bachant, T. Käufer, jakirkham, A. Bauer, B. Vodenicharski, C. Dallas, J. Borg, tomerast, and ranleu, OpenPIV (2020).